AFRL-PR-WP-TP-2006-249

UPSTREAM MIXING CAVITY COUPLED WITH A DOWNSTREAM FLAMEHOLDING CAVITY BEHAVIOR IN SUPERSONIC FLOW (POSTPRINT)

Adam Quick, Paul I. King, Mark R. Gruber, Campbell D. Carter, and Kuang–Yu Hsu

JULY 2005

Approved for public release; distribution is unlimited.

STINFO COPY

PROPULSION DIRECTORATE
AIR FORCE MATERIEL COMMAND
AIR FORCE RESEARCH LABORATORY
WRIGHT-PATTERSON AIR FORCE BASE, OH 45433-7251

REPORT DOCUMENTATION PAGE

Form Approved
OMB No. 0704-0188

1. REPORT DATE *(DD-MM-YY)*	2. REPORT TYPE	3. DATES COVERED *(From - To)*
July 2005	Conference Paper Postprint	09/01/2004 – 07/31/2005

4. TITLE AND SUBTITLE
UPSTREAM MIXING CAVITY COUPLED WITH A DOWNSTREAM FLAMEHOLDING CAVITY BEHAVIOR IN SUPERSONIC FLOW (POSTPRINT)

5a. CONTRACT NUMBER
In-house

5b. GRANT NUMBER

5c. PROGRAM ELEMENT NUMBER
62203F

6. AUTHOR(S)
Adam Quick and Paul I. King (Air Force Institute of Technology)
Mark R. Gruber and Campbell D. Carter (AFRL/PRAS)
Kuang–Yu Hsu (Innovative Scientific Solutions, Inc.)

5d. PROJECT NUMBER
3012

5e. TASK NUMBER
AI

5f. WORK UNIT NUMBER
00

7. PERFORMING ORGANIZATION NAME(S) AND ADDRESS(ES)

Air Force Institute of Technology
WPAFB, OH 45433

Propulsion Sciences Branch (AFRL/PRAS)
Aerospace Propulsion Division
Propulsion Directorate
Air Force Research Laboratory
Air Force Materiel Command
Wright-Patterson AFB, OH 45433-7251

Innovative Scientific Solutions, Inc.
Dayton, OH 45440

8. PERFORMING ORGANIZATION REPORT NUMBER
AFRL-PR-WP-TP-2006-249

9. SPONSORING/MONITORING AGENCY NAME(S) AND ADDRESS(ES)

Propulsion Directorate
Air Force Research Laboratory
Air Force Materiel Command
Wright-Patterson AFB, OH 45433-7251

10. SPONSORING/MONITORING AGENCY ACRONYM(S)
AFRL-PR-WP

11. SPONSORING/MONITORING AGENCY REPORT NUMBER(S)
AFRL-PR-WP-TP-2006-249

12. DISTRIBUTION/AVAILABILITY STATEMENT
Approved for public release; distribution is unlimited.

13. SUPPLEMENTARY NOTES
Conference paper published in the Proceedings of the 41st AIAA/ASME/SAE/ASEE Joint Propulsion Conference and Exhibit, published by AIAA.

The U.S. Government is joint author of the work and has the right to use, modify, reproduce, release, perform, display, or disclose the work. PAO case number: AFRL/WS 05-1437; Date cleared: 16 Jan 2005. Paper contains color.

14. ABSTRACT
Experimental investigations of the flowfield associated with three upstream direct injection acoustic resonance cavities coupled with a previously designed downstream combustion cavity in a non-reacting flow are described. All of the upstream mixing cavities were acoustically open (shear layer reattachment on the downstream wall of the cavity) with the length-to-depth ratio (L/D) on the order of 1. The previously established downstream combustion cavity had an L/D of 4.7 and an aft ramp angle of 22.5 degrees. The three upstream mixing cavities were characterized in Mach 2 freestream flow with injection at three locations (upstream wall, center, downstream wall) within each cavity. Injection at the upstream wall of the cavity provided greater penetration height into the freestream as well as faster mixing with the freestream compared with injection at the center or downstream wall of the cavity. Injection at the center of the cavity resulted in the injectant diffusing laterally in the cavity before being ejected into the freestream. Injection at the downstream cavity wall displayed characteristics of both injection at the upstream wall and center of the cavity.

15. SUBJECT TERMS
Supersonic combustion, fuel injection, laser-based diagnostics

16. SECURITY CLASSIFICATION OF:			17. LIMITATION OF ABSTRACT:	18. NUMBER OF PAGES	19a. NAME OF RESPONSIBLE PERSON (Monitor)
a. REPORT	b. ABSTRACT	c. THIS PAGE			Mark R. Gruber
Unclassified	Unclassified	Unclassified	SAR	20	19b. TELEPHONE NUMBER *(Include Area Code)* N/A

Standard Form 298 (Rev. 8-98)
Prescribed by ANSI Std. Z39-18

41st AIAA/ASME/SAE/ASEE Joint Propulsion Conference & Exhibit
10 - 13 July 2005, Tucson, Arizona

AIAA 2005-3709

Upstream Mixing Cavity Coupled with a Downstream Flameholding Cavity Behavior in Supersonic Flow

Adam Quick[*] and Paul I. King.[†]
Department of Aeronautics and Astronautics
Air Force Institute of Technology, Wright-Patterson AFB, OH, 45433

Mark R. Gruber[‡] and Campbell D. Carter[§]
Propulsion Directorate, Propulsion Sciences Branch
Air Force Research Laboratory, Wright-Patterson AFB, OH, 45433
and

Kuang-Yu Hsu[**]
Innovative Scientific Solutions, Inc., Dayton, OH, 45440

Experimental investigations of the flowfield associated with three upstream direct-injection acoustic resonance cavities coupled with a previously designed downstream combustion cavity in a non-reacting flow are described. All of the upstream mixing cavities were acoustically open (shear layer reattachment on the downstream wall of the cavity) with the length-to-depth ratio (L/D) on the order of 1. The previously established downstream combustion cavity had an L/D of 4.7 and an aft ramp angle (Θ) of 22.5 degrees. The three upstream mixing cavities were characterized in Mach 2 freestream flow with injection at three locations (upstream wall, center, downstream wall) within each cavity. Injection at the upstream wall of the cavity provided greater penetration height into the freestream as well as faster mixing with the freestream compared with injection at the center or downstream wall of the cavity. Injection at the center of the cavity resulted in the injectant diffusing laterally in the cavity before being ejected into the freestream. Injection at the downstream wall of the cavity displayed characteristics of both injection at the upstream wall and center of the cavity. The flow over the downstream cavity was similar for all injection locations. Pressure taps along the ceiling and floor of the test section showed no distinct change in pressure readings due to either cavity length or injection location within the cavity.

Nomenclature

AFRL	=	Air Force Research Laboratory
D	=	depth of cavity
FFT	=	fast Fourier transform
IR	=	infrared
L	=	length of cavity
L/D	=	length to depth ratio
Nd:YAG	=	neodymium doped yttrium-aluminum-garnet
NO	=	nitric oxide
PLIF	=	planar laser induced fluorescence
SLPM	=	standard liters per minute
Θ	=	downstream wall or ramp angle

[*] Capt, USAF, Master's student, Nonmember.
[†] Professor, Senior Member.
[‡] Senior Aerospace Engineer, Associate Fellow.
[§] Senior Aerospace Engineer, Associate Fellow.
[**] Research Scientist, 2766 Indian Ripple Rd., Associate Fellow.

I. Introduction

One of the critical technologies needed for the continuation of the United States' air and space superiority is hypersonic air-breathing propulsion vehicles. Such vehicles will be used for reconnaissance and payload delivery through the use of cruise missiles or manned and unmanned aircraft. Hypersonic aircraft will also provide affordable and relatively fast access to space. The speeds reached by hypersonic vehicles (Mach 5 or greater) will greatly improve the time critical intelligence gathering and strike capability of our nation's military. In addition, the increased kinetic energy of hypersonic vehicles will improve the performance of penetration weapons and warheads.

A. Background

One of the options for the propulsion system of a hypersonic vehicle is an air-breathing Supersonic Combustion Ramjet or Scramjet. The United States has an ongoing research effort into the subject, through the National Air and Space Administration (NASA), private industry, and several agencies in the Department of Defense (DoD), such as the Defense Advanced Research Project Agency (DARPA) with its Force Application and Launch from CONUS (FALCON), the Navy's Rapid Response Missile Program, the Army Scramjet Technology Program, and the Air Force with the Air Force Research Laboratory (AFRL) Propulsion Directorate's Hypersonic Technology (HyTech) Program.[1]

As the velocity of the free stream air through the scramjet increases, a longer combustion chamber is needed to increase the residence time of the oxygen, allowing the fuel-oxidizer mixing and combustion process to complete prior to exiting through the expansion nozzle of the engine. However, increasing the length of the combustion chamber increases the overall weight of the aircraft and the drag as well as the thermal losses, reducing the efficiency of the engine. As a result, a short combustion chamber is desired for scramjet engines. The need arises for small combustion chamber designs that minimize fuel-air mixing time while sustaining a complete combustion process within the chamber and minimize the drag, pressure, and thermal losses of the engine.

B. Previous Research

Three general techniques for flameholding and flame stabilization in scramjet engines have been developed and investigated.[2] One of the first techniques studied for flameholding and mixing is achieved using the organization of a recirculation area that allows fuel and air to be mixed at subsonic velocities. Controlled interaction of a shock wave with mixed fuel and oxidizer is another method investigated for flameholding and stabilization. The final technique is the formation of unmixed fuel and air structures which allow a diffusion flame to occur as the fuel-oxidizer structures move downstream.

The simplest approach to mix fuel with the freestream air in a scramjet combustor is direct transverse injection or angled injection of fuel.[2] As the fuel jet interacts with the supersonic freestream flow, a bow shock is produced. This causes the upstream shear layer to separate, which in turn creates a subsonic mixing region and combustion region upstream of the fuel jet. The transverse injection resulting bow shock can be strong, and may result in relatively large total pressure losses through the chamber.[2] The angled injection bow shock is weaker than that of transverse injection and results in comparatively less total pressure losses; however, the mixing and stable combustion region is typically smaller.[2]

The next iteration of flameholding, flame stabilization and mixing incorporates a step on the combustion chamber floor.[2] At the base of the step, fuel is transversely injected. This step creates a longer recirculation zone for mixing and combustion compared to that of direct injection or angled injection into the freestream flow. The hot gases from the combustion process also serve as a continuous ignition source. This method results in relatively high total pressure losses as a combined bow and step-induced shock form near the injection port.[2]

Acoustic actuators have been shown to significantly alter subsonic flow fields and greatly increase shear layer growth rates.[3] Subsonic acoustic actuators in supersonic flows are less effective due to the stability characteristics of compressible shear layers. Compressible shear layers are found to be poorly organized and strongly three dimensional, making it extremely difficult to induce and maintain organized structures and properties for communication downstream in the flow field.[3] Typical supersonic flows require high frequency excitation which most subsonic actuators can not provide. One acoustic actuator found suitable is the inclusion of acoustic resonance cavities adjacent to the supersonic flow field.[3]

Acoustic cavities provide a method to excite supersonic flows to the point of significant change in the mixing characteristics of shear flow. Cavity induced oscillations in turbulent compressible shear layers demonstrate the ability to manipulate the fuel-air mixing rate and change the combustion characteristics downstream of the resonance cavity.[3]

Incorporation of acoustically open cavities on the walls of the scramjet combustion chamber provides a relatively large and stable region for mixing and flameholding. An acoustically open cavity is defined to have a length-to-depth (L/D) ratio, generally less than 10, such that the shear layer reattaches to the downstream wall of the cavity, not the floor. An acoustically closed cavity is defined to have an L/D ratio sufficiently large enough (greater than 10) that the shear layer reattaches to the cavity floor.[4] Investigations demonstrate closed cavities have a much higher drag penalty than open cavities.[2] The pressure losses through the combustion chamber due to the open cavity are relatively small. The existence of the cavity allows a small region for subsonic fuel-air mixing and combustion to exist adjacent to the supersonic freestream flow.[4]

Open cavities with L/D on the order of unity create sustained oscillations in the transverse mode (Fig. 1).[5] As the free-stream air flows over the cavity, a vortex is shed from the leading edge of the cavity. Eventually, the vortex fills the cavity and entrains mass from the freestream, compressing the gas trapped beneath it. The increased pressure created from the entrainment and compression ejects the vortex into the free-stream flow. A new vortex forms and leads to self-sustained oscillations in the cavity. The frequency of the ejected vortices is controlled by the flow conditions and dimensions of the cavity.

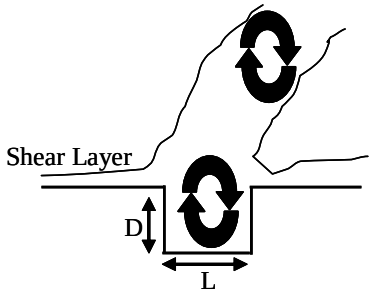

Figure 1. Transverse oscillation mode.

Open cavities with an L/D ratio greater than unity oscillate in the longitudinal mode (Fig. 2).[5] A large vortex is found to stabilize near the downstream wall of the cavity. This organized structure moves in the transverse direction controlling the inflow of mass and momentum to the cavity at the trailing edge. The trailing edge vortex is replenished by a continuous series of vortices shed from the leading edge of the cavity. An acoustic compression wave is created by the impingement of the shear layer on the downstream wall of the cavity. This wave reflects from the upstream wall, travels downstream deflecting the shear layer, allowing the mass entrained in the cavity by the trailing edge vortex to escape.[2]

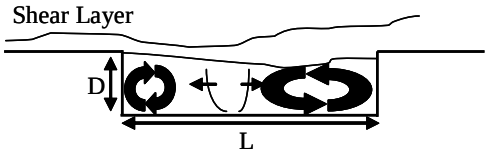

Figure 2. Longitudinal oscillation mode.

In order for a cavity to operate as a stable flame holder, the cavity must demonstrate suitable performance in such areas as static pressure within the flame holder, entrainment rate, residence time, and drag. The cavity must also show acceptable performance across a range of operating conditions, such as those experienced in a dual-mode scramjet. In a dual-mode scramjet, a relatively strong pressure rise inside the combustion chamber exists at ignition and relatively low flight Mach numbers.[6] The energy added to the freestream flow from the combustion process causes the approaching supersonic flow to decelerate through a series of shock waves, increasing the static pressure and slowing regions of flow in the combustion chamber to subsonic speeds. This combination of supersonic and subsonic flows experienced by the chamber over the flight envelope is designated dual-mode operation. As the flight Mach number increases, the shock-train weakens and the flow through the combustion chamber returns to completely supersonic speed. In the test environment, the shock train is created by raising the backpressure of the test section.[6]

Acoustically open cavities are the main research interest for dual-mode scramjet flameholding due to the lower drag penalty compared to acoustically closed cavities. Cavities with lower L/D ratios (L/D<2) lack enough volume for flameholding, while a cavity with too high an L/D ratio produces unstable flames. This drives research into a longitudinal oscillation mode, acoustically open flame-holding cavity. L/D ratios on the order of 3-5 have been demonstrated to be acceptable flameholders.

To stabilize the flame inside the cavity, a means to steady the cavity flow is needed. One solution discovered to aid in stabilization is decreasing the wall or ramp angle (θ) of the downstream wall of the cavity.[7] Decreasing the ramp angle creates a more acoustically stable cavity flow and in turn creates a more stable region for the combustion process. Entrainment of the freestream into the cavity also increases because the shear layer impinges deeper into the cavity. The resultant drag on the downstream surface of the cavity increases because the relatively high pressure of the shear layer acts on a larger surface area. Another limitation discovered is that the residence time of the fuel-air mixture within the cavity decreases as the aft ramp angle decreases. Cavities with small ramp angles exhibit one primary recirculation zone and exchange mass more freely with the freestream compared to cavities with larger ramp angles that exhibit the secondary vortex structure near the leading wall. The strong interdependence of all flow characteristics in the flameholding cavity had to be taken into account to provide a robust design.[7]

Research at the Propulsion Sciences Branch (PRAS) of AFRL led to the design of a dual-mode flameholding cavity with a depth of 0.65 inches, and overall length of 3.08 inches (L/D = 4.7) and a ramp angle of 22.5 degrees (Fig. 3). Several fueling schemes for the cavity tested included injection upstream of the cavity which allowed entrainment of fuel and air into the cavity as well as direct cavity fueling with the necessary oxidizer entrained from the freestream. The direct cavity fueling methods injected fuel at one of two locations, from the floor of the cavity near the upstream wall, and from the downstream ramp of the cavity. Injection from the ramp of the cavity was the only fueling scheme that demonstrated sustained combustion throughout dual-mode operation.[6]

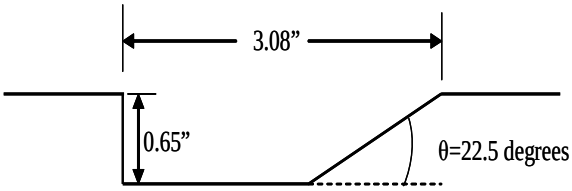

Figure 3. AFRL/PRAS dual mode flame holding cavity.

Acoustic resonance cavities placed in tandem in supersonic flow have been shown to have great influence on each other.[8] When a cavity precedes another, the flow over the downstream cavity is strongly affected by the upstream cavity through modifications in the shear layer. The interaction between two cavities in tandem is driven by the type and streamwise location of each cavity.

When a cavity dominated by the transverse oscillation mode is paired with another cavity of the same dimensions, the basic flow features of the downstream cavity are not greatly affected. The oscillatory frequencies of the upstream cavity are found in the downstream cavity as well as downstream of each cavity on the test section floor. Any high frequency modes are damped in the downstream cavity while the dominant mode inside the cavity is enhanced. The shear layer experiences a slight increase in thickness after each cavity. When a cavity dominated by the longitudinal mode is paired with another cavity of the same type, the upstream cavity was shown to set the phase of the oscillations in the downstream cavity. The increased mixing level in the shear layer caused by the oscillation in the cavity was found to increase the boundary layer thickness significantly. Any disturbances generated by the upstream cavity were amplified by the downstream cavity.[8]

C. Current Study

The following sections describe recent efforts to obtain additional information of the fluid-mechanic characteristics of direct-injection acoustically open resonance cavities and the effects on the downstream combustion chamber. The primary goal of this experiment was to characterize the mixing effectiveness of an upstream cavity coupled with fuel injected at different locations inside the cavity. The secondary goals were to determine the effect on static pressure through the test section by the inclusion of the upstream cavity and the injectant as well as to determine if the acoustic characteristics of the upstream cavity were carried downstream by the shear layer to the downstream combustion cavity, raising the shear layer higher into the free stream and creating a greater ignition area for the freestream fuel-air mixture. Advanced visual and pressure diagnostics were used to collect the data necessary to improve the understanding of the flowfield-injectant interactions.

II. Experimental Setup

A. Test Facility

The AFRL/PRAS Large-Scale Supersonic Combustion Research Facility is an in-house facility capable of allowing studies of the enhancement and control of fuel-air mixing in supersonic combustors with conventional and state-of-the-art non-intrusive diagnostic techniques. The tunnel design provides optical access from three sides of the test section through fused silica windows which provide excellent transmissive properties in the ultraviolet wavelengths. The nozzle sidewalls, as well as the top and bottom walls of the test section are equipped with conventional static pressure and thermocouple taps. Further details of the test facility are described elsewhere.[9]

A two-dimensional converging-diverging Mach 2 nozzle section, configured with an asymmetric nozzle, is used to develop the desired inlet conditions. The facility nozzle is configured with nozzle blocks to create a 2-inch high by 6-inch wide exit to create the Mach 2 flow through the test section. The test section is equipped with inserts to create a constant-area isolator section 7 inches in length. The constant area isolator allows the tunnel to function in ramjet, scramjet and dual modes. In the ramjet configuration, the backpressure is raised to move the shock structure completely into the isolator section creating purely subsonic flow in the test section. Lowering the backpressure moves the shock structure into the test section. Lowering the backpressure further creates purely supersonic flow in

the test section. The isolator section is followed by an insert creating an expansion section diverging at 2.5 degrees 29.125 inches in length.

B. Test Procedure

The three upstream mixing cavities are flush-mounted to the divergent ramp individually upstream of the combustion cavity (Fig. 4). All three cavities have the same general dimensions except for the streamwise length of the cavity. Each cavity is 1.0 inches deep by 2.34 inches wide in the spanwise direction. The three cavities have streamwise lengths of 0.75 inches, 1.00 inches, and 1.25 inches, respectively (L/D = 0.75, 1.00, and 1.25). These cavities are acoustically open and designed to create transverse oscillations to enhance injectant mixing with the freestream with less total pressure loss compared to injection on the test section floor. Each cavity floor has three injection ports in three streamwise locations along the cavity. The injection port locations are tangent to the leading edge, the center of the cavity, and tangent to the downstream wall of the cavity.

Pressure Systems, Inc. (PSI) pressure transducers and Type-K thermocouples are connected along the nozzle and test section per the facility's standard operating procedure. Data are recorded once per second for 10 seconds for each test condition. Kulite XT-190 series high frequency response pressure transducers with a pressure range of 0-50 PSIA are installed for collection of high-frequency pressure oscillations inside the upstream cavities and the downstream combustion chamber. The pressure was sampled at 100 kilohertz (kHz). All components are connected to the AFRL/PRAS developed in-house data acquisition system consisting of off-the-shelf subsystems.

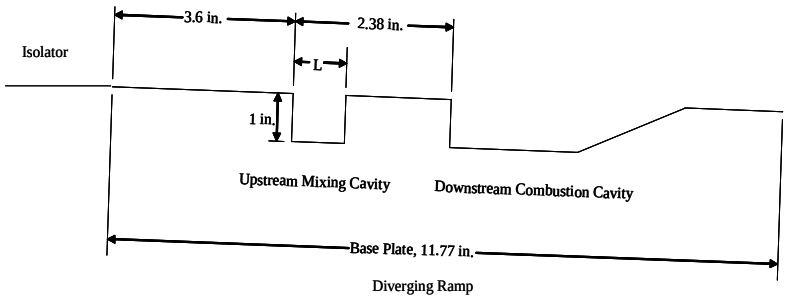

Figure 4. Divergent ramp schematic.

The flow through the test section is then allowed to stabilize at one of two backpressure conditions. The high back pressure setting simulates the ignition transient at low Mach numbers, creating a shock-train and a mixed supersonic-subsonic flow in the test section. The low backpressure condition simulates higher Mach numbers where the shock-train weakens and the freestream flow returns to supersonic. The low backpressure setting is the operating condition of interest as previous research shows greatly increased mixing at the high-backpressure setting.

For each run, two of the upstream cavity injection taps are capped while the third is connected to the facility's nitric oxide (NO) gas injection system. A dome loader, controlled remotely with an air-actuated isolation valve, regulates the injection pressure into the cavity. The gas is injected at three pressures (50, 100, 200 PSIG) per injection location.

C. Planar Laser-Induced Fluorescence (PLIF) Diagnostics

NO-PLIF is used to track the penetration height and width of the injection plume visually at various locations downstream. A supply of air is seeded with NO-doped N_2 (10,000 ppm NO mole fraction) to simulate fuel injection into the cavity. A Millipore Tylan 2925 Series Mass Flow Controller of 500 Standard Liters Per Minute (SLPM) controls the seeding prior to injection. The fraction of NO/N_2 is relatively low, so that the net electronic quenching rate is roughly independent of the mixture fraction of the injectant. This allows the intensity of the fluorescence to be correlated with the concentration of the NO regardless of the observed position in the flow. Increasing the injection pressure requires more NO-doped N_2 mixed with the air prior to injection to maintain comparable intensities between injection pressures.

For laser diagnostics using the NO-PLIF technique, a Lumonics Hyperdye dye laser is pumped with the second harmonic of an injection-seeded Spectra Physics Nd:YAG laser (GCR-170). The dye laser output is frequency-doubled using an Inrad Autotraker III. To generate the wavelength for NO excitation, a second Autotraker III is employed where the doubled-dye beam is frequency-mixed with the residual infrared (IR) beam from the Nd:YAG. For NO excitation, the dye laser is set to a wavelength of 574 nm to produce frequency-mixed radiation at 226 nm.

To generate the wavelength for NO excitation, a second Autotraker III is employed where the doubled-dye beam is frequency-mixed with the residual infrared (IR) beam from the Nd:YAG. For NO excitation of the $R_1(6.5)$ transition of the $A^2\Sigma^+ (v' = 0) \leftarrow X^2\Pi_i (v'' = 0)$ band, the dye laser is set to a wavelength of 574 nm to produce frequency-mixed radiation at 226 nm. The pump beam energy and wavelength are continuously monitored (with an

oscilloscope) using a photodiode (for the energy) and the combination of a reference flame, to produce NO, and a photomultiplier tube (to detect the LIF signal).

The laser sheet is formed using a pair of lenses, a plano-concave cylindrical lens (-50 mm [CDC1]focal length) and a plano-convex spherical lens (1000 mm focal length). This arrangement results in a sheet height of approximately 3 inches. The transmitting and receiving optical hardware are positioned on a traversing table allowing remote positioning of the measurement volume at any desired station in the flow field.

A Princeton Instruments PIMAX Charge-Coupled Device (CCD) digital camera with a 512 by 512 pixel array, which was binned 2 by 2, is employed to record NO PLIF images. For the end-view imaging a Nikon 105-mm f/4.5 UV lens—fitted with a single Schott glass UG-5 filter to transmit fluorescence from the (0,1), (0,2), (0,3)… bands and block scattering at 226 nm—was employed; for side-view imaging a Cerco 45-mm f/1.8 lens was employed along with the UG-5 filter. Because images are collected at the laser repetition rate, 10 Hz, they are not time correlated.

The profile or cross-flow visualization places the laser sheet on the center line of the test section. End view images are collected at the upstream wall, center, and downstream wall of each cavity as well as 2 inches downstream from the leading edge. Because of limited visual access through the end of the test section, the camera is place at an angle to the side window of the test section. Perspective image distortion—a result of off-axis imaging—is corrected using a calibration image (an array of dots).

III. Results and Discussion

A. Visual Data Analysis

NO-PLIF provided a visual measure of both the concentration (mean images) of the NO injected into the cavity and its mixing potential (standard deviation images) with the freestream. Images with 200 PSIG injection pressure are shown because of the relatively high concentration of NO in the injected gas maintaining image contrast as the injectant progressed downstream. The cavity with a length of 1.25 inches is chosen as the representative for the entire study. The concentration is represented by the mean of the sequences of images collected during each test run at each downstream location. Brighter areas in the concentration images are areas of high concentration (an 8-bit linear gray scale is employed). The mixing potential is represented by the standard deviation images (also an 8-bit gray scale) created from the sequences collected. Brighter areas in the image are of relatively high standard deviation, or fluctuation, in the image. Areas of high fluctuation in NO concentrations indicate potential areas of high NO-air mixing.

Three distinct behaviors of the mixing cavities are found based on the injection location within the cavity. Injection at the forward wall resulted in a well organized plume that lifted relatively high into the freestream in a relatively short distance. The plume began with a very highly concentrated area of NO just above the test section floor at the leading edge of the cavity on the center line. As the flow progressed downstream to the midpoint of the cavity, the concentration has dropped considerably as the NO began to diffuse into the shear layer and freestream.

At the trailing edge of the cavity, or 1.25 inches downstream of the injection port, a very well-defined plume took shape. A relatively high concentration of NO was observed centered just below the top of the plume, extending around the center of the plume. The concentration increased radially from the outside edge of the plume toward the center and then decreases rapidly near the center. The plume maintained its shape and structure 2 in. downstream of the injection port (Fig. 5).

The standard deviation images showed the most concentrated mixing potential at the leading edge of the cavity. As the NO-laden gas progressed downstream the mixing rate dropped considerably with freestream/shear layer mixing. The areas of highest mixing potential coincided with the areas of highest concentration represented by the brightest locations in the image. The standard deviation increased radially inward toward the center of the plume and then decreased rapidly near the center forming a mixing band that matches the concentration band (Fig. 6).

The characteristic behavior demonstrated by injecting into the center of the cavity created a layer of relatively equally diffused NO spanning the width of the

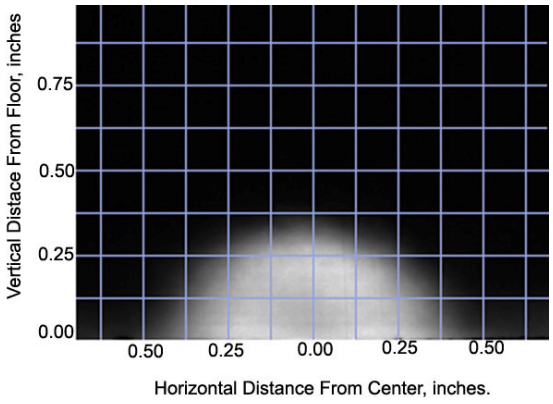

Figure 5. Upstream wall injection mean image 2 inches downstream of cavity leading edge.

image (Fig. 7). This suggested mixing inside the cavity prior to the injectant being expelled or injectant trapped inside the cavity unable to escape into the freestream. Again this behavior was not significantly altered with injection pressure.

Unlike with injection at the upstream wall, no injectant was visible at the leading edge of the cavity. The NO did not propagate upstream in high enough concentrations while inside the cavity to be observed at the leading edge.

The midpoint of the cavity was directly above the injection port. Even at 200 PSIG injection pressure, the characteristics of the cavity's flow dominated the diffusion of the NO above the test section floor. Unlike the plume from upstream wall injection, middle injection produced a very low concentration band of NO spanning the width of the image. Injection in the center of the cavity provided a relatively large volume for the injected fluid to be suppressed. The injectant could disperse radially in all directions from the port in response to flow characteristics. Injection at the upstream wall or downstream wall limited the radial dispersion. A very high concentration of NO was just above the test section floor over the cavity.

As the flow progresses downstream to the trailing edge of the cavity, the band of NO remained in relatively low concentration but gradually lifted above the test section floor. The concentration image in Fig. 7 was collected 2 inches downstream of the leading edge of the cavity and shows that the concentration of NO continued to slowly grow in height and maintained its width. The areas of highest concentration remained near the cavity floor. The band was not as level as it was upstream with the middle of the band becoming higher faster than the edges. This was most likely due transverse momentum from the injection pressure in the middle of the layer of NO.

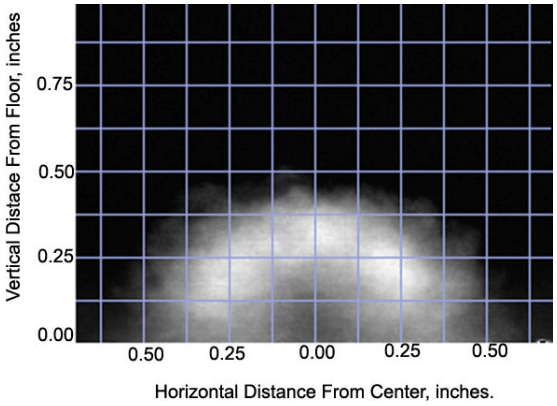

Figure 6. Upstream wall injection standard deviation image 2 inches downstream of cavity leading edge.

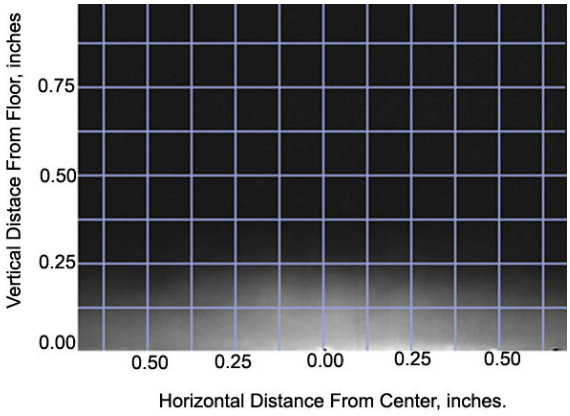

Figure 7. Center injection mean image 2 inches downstream of cavity leading edge.

Again the standard deviation images coincided with the concentration images. There was no mixing at the leading edge. At the midpoint, the highest level of mixing was over the injection port at the center of the cavity. However, the mixing rates near the edges of the image were relatively high, demonstrating a substantial mixing region along the entire width of the cavity.

As the flow progressed downstream to the trailing edge of the cavity, less mixing occurred, but it was more evenly spread throughout the layer of NO, with the highest region of mixing lifting higher into the band. The mixing region maintained the same height across the width of the cavity compared to the concentration images where a peak near the center of the cavity was clearly visible.

At the 2 in. location downstream of the leading edge, the mixing was fairly constant along the entire width and height of the band (Fig. 8). However, the mixing rate was lower than the previous location. The overall height of the band had increased slightly between the previous and current locations.

Injection at the downstream wall of the cavity provided no visible concentration of NO at the leading

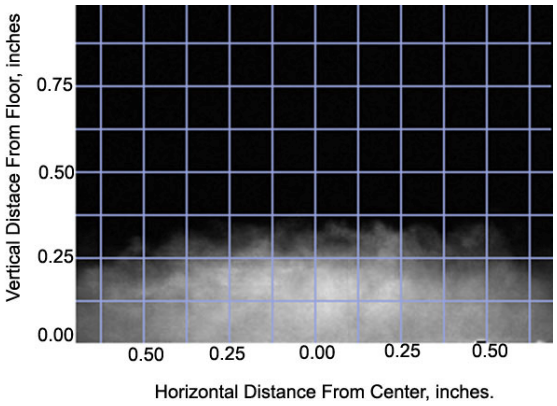

Figure 8. Center injection standard deviation image 2 inches downstream of cavity leading edge.

edge of the cavity. However, unlike middle injection, NO was visible upstream of the injection port. A thin layer of relatively uniform concentration NO spanned the width of the image taken at the midpoint of the cavity. The mechanism inside the cavity allowing the NO to mix with the shear layer upstream of the injection point was most likely a trapped vortex.

At the trailing edge of the cavity, the concentration of NO was high enough to wash out the lower concentrations spanning the width of the image. Only a small plume over the center of the cavity was observed. The height of the plume was hard to judge because of the high concentration level just above the surface of the test section. At the 2 in. point downstream of the leading edge of the cavity, a clear peak of relatively high concentration NO was seen overlaying the band of NO spanning the width of the image (Fig. 9). The injection momentum was strong enough to overcome the strength of the vortex and be carried downstream with the flow once outside the cavity.

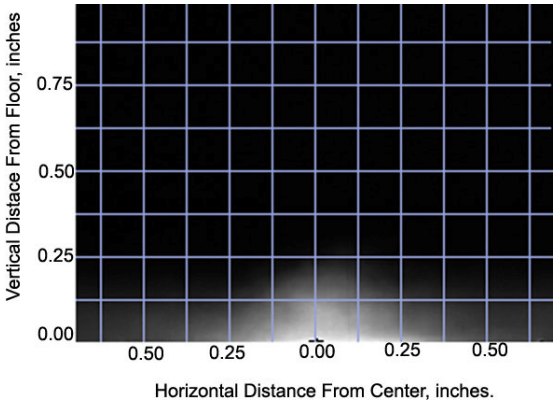

Figure 9. Downstream wall injection mean image 2 inches downstream of cavity leading edge.

The standard deviations showed trends consistent with the concentration images. No mixing was visible at the upstream wall of the cavity. Very little mixing was seen at the midpoint of the cavity. The highest level of mixing occurred in the plume formed above the injection port on the downstream wall. The mixing in the band that spanned the width of the image was washed out by the high mixing potential in the plume. By 2 in. downstream of the leading edge of the cavity most of the mixing was localized in the plume moving downstream (Fig. 10).

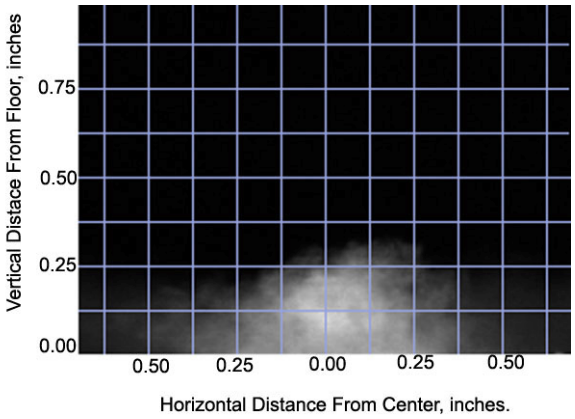

Figure 10. Downstream wall injection standard deviation image 2 inches downstream of cavity leading edge.

The images that every test condition has in common were collection at the leading edge of the cavity and 2 inches downstream of the leading edge. Significant concentration areas and significant mixing areas are found for the 200 PSIG injection condition for every cavity and injection location at the low backpressure setting. Significant areas are created to compare the diffusion rates and mixing potentials of the test conditions.

Each image was set to the same palette scale. All the images were then imported into Adobe Photoshop to find the 50% value of the maximum pixel brightness. All pixels within 50% of the maximum brightness were added together. The pixels were then converted to square inches to find the desired area. The results are presented in Table 1.

Table 1. Significant concentration and mixing areas

Cavity Length (in)	Port	Concentration Area (sq. in.)	Mixing Potential Area (sq. in.)
0.75	Aft	0.03	0
0.75	Middle	0.06	0
0.75	Forward	0.02	0
1.00	Aft	0.04	0
1.00	Middle	0.03	0
1.00	Forward	0.02	0
1.25	Aft	0.05	0.05
1.25	Middle	0.10	0
1.25	Forward	0.01	0

Injecting into the upstream wall port leads to the lowest concentration areas because a longer distance was covered. The 1.25 in. cavity had a significantly smaller area compared to the other two cavities. Injection into the center port kept the NO near the cavity floor, prevented mixing and leading to a larger area. Downstream port injection created a larger surface for diffusion in the vertical direction compared to middle injection. Downstream port injection had the shortest mixing time, and resulted in a significant mixing potential area for the 1.25 in cavity, and a higher significant area for the 1.00 in. cavity compared to injection at the center port.

For the high back pressure test conditions the injected NO mixes very rapidly in the transverse direction with the freestream due to the increased static pressure and flow field distortions over the cavity from the shock-train. A mean image showing 200 PSIG injection at the upstream port was collected 2 in. downstream of the leading edge of the 1.25 in. cavity and is provided for comparison to the low backpressure test conditions in Fig. 11. The results are representative of all high backpressure tests. High backpressure conditions are an advantageous mixing environment simulating the ignition transient of a scramjet at low flight Mach numbers. However, a scramjet does not operate in this regime for any appreciable amount of time.

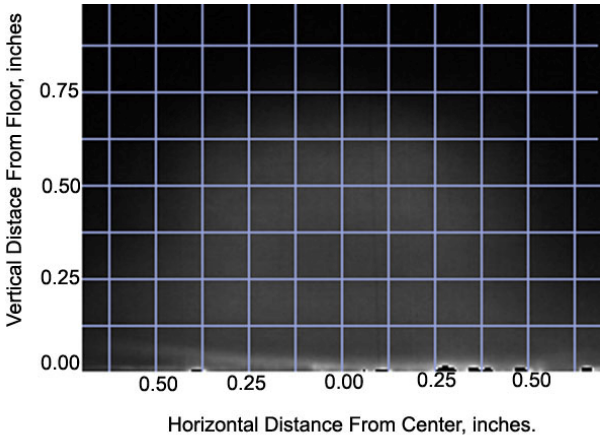

The behavior with upstream injection location and the effect on the flow over the combustion cavity was demonstrated in the profile views of collected for each cavity. Figure 12 is a compilation of the mean images taken at each injection site for 200 PSIG injection pressure at each of the three injection ports inside the 1.25 in. cavity. The camera remained centered in the same location for each image. The palette scales for the images are identical, and the image plane was located at the center of the cavity.

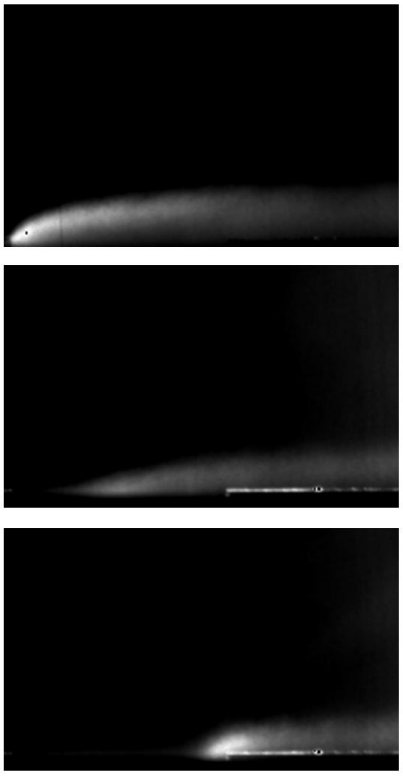

Each side-view image confirmed the information provided from the end-view images. Injection at the leading edge of the cavity lifted the NO into the test section without apparent interference from the flow characteristics within the cavity. The highest concentration was at the leading edge of the cavity just above the test section floor. The mean image did not suggest that vortices trapped in, or ejected from, the cavity had any substantial effects on the behavior of the injected flow. The injected fluid did not appear to be aided by the upward momentum of a trapped vortex in the cavity in the mean.

The mean image with center injection confirms that the cavity did not allow high concentrations of NO to continuously transition from the cavity to the test section flow. The image shows a layer of uniformly concentrated NO being lifted out of the cavity. The growth rate in the transverse direction (height-wise) was not as rapid as injection at the leading edge of the cavity.

The downstream wall injection image illustrates that on the average, the transverse momentum of the injected jet could overcome any opposing momentum from a trapped vortex within the cavity. A no slip condition at the downstream wall of the cavity may have lessened the downward momentum effects over the injection port for any vortex in the cavity.

As with the end view images, the highest standard deviations and in turn potential mixing rates coincided with the areas of highest concentrations (Fig. 13). For upstream wall injection, the highest levels of mixing spread both

downstream and transversely in the flow. The image suggests that the NO mixes mostly with the shear layer and freestream as the band of mixing lifts above the cavity as it travels downstream. No mixing is apparent at the trailing edge of the cavity.

The standard deviation images in the center injection scenario suggest two possibilities. One is the injectant was suppressed from moving transversely into the freestream by the flow characteristics of the cavity which lead to a slower potential mixing rates. Another is the injectant mixed inside the cavity with the entrained air and then escaped into the freestream. Entrainment into the freestream appeared to be more gradual compared with injection at the forward wall. NO was seen at the leading edge of the cavity but has not entered the shear layer. The transverse momentum of the injected flow appeared to be suppressed by the flow characteristics of the cavity.

Downstream wall injection produced very strong localized mixing potential at the trailing edge of the cavity. Like center injection, very faint indications of NO mixing with air in the cavity up to the leading edge exist in the image.

The mixing appeared to grow linearly into the freestream until it reached the trailing edge of the cavity where the momentum from the injection began to dominate the local flow. Just downstream of the injection port the mixing potential became more uniform.

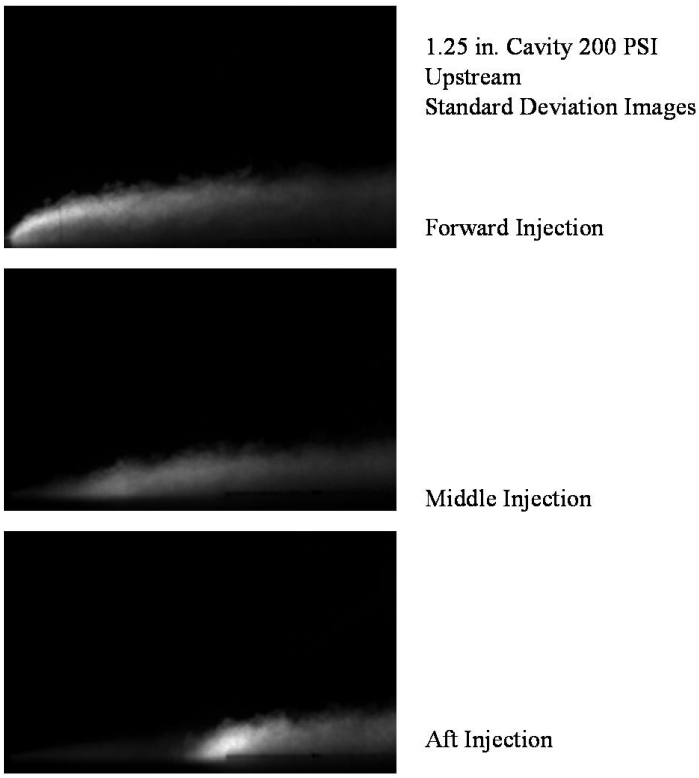

Figure 14 contains the mean profile images for the effects on the downstream cavity with 200 PSIG injection pressure at the three upstream cavity locations inside the 1.25 in. cavity. Once the flow encountered the leading edge of the downstream cavity the NO was lifted higher into the freestream with upstream wall injection. Injection at the center and downstream wall locations did not demonstrate the same NO growth over the cavity. Both center and downstream wall injection showed high concentration levels of NO in the flow over the downstream cavity with downstream wall injection showing the highest of the three. This is consistent with the end view images as downstream wall injection had less time to mix with the freestream flow. All three injection locations allowed NO to be entrained into the combustion cavity.

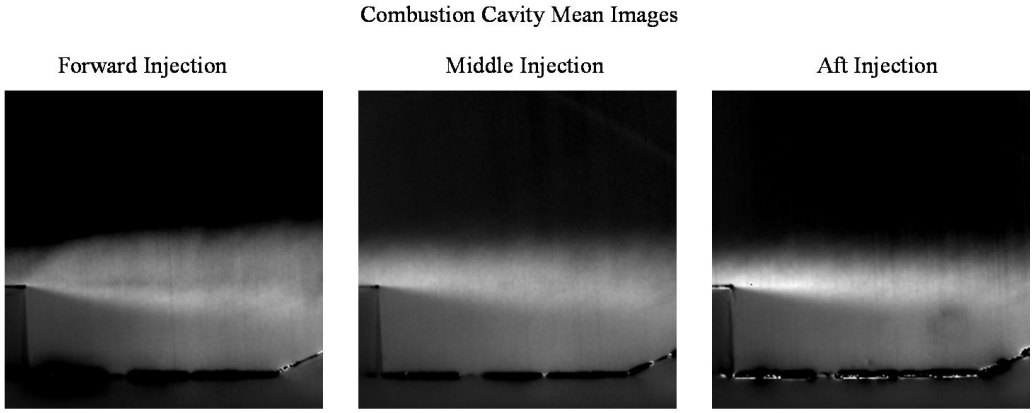

Figure 14. Mean profile images of downstream combustion cavity for each injection location

The standard deviations for the above images are contained in Fig. 15. Forward injection had the largest area of mixing potential while aft injection had the highest potential mixing rate. There was very little mixing potential observed within the cavity, indicating a higher mixing rate in the cavity resulting in a well mixed medium compared to the freestream.

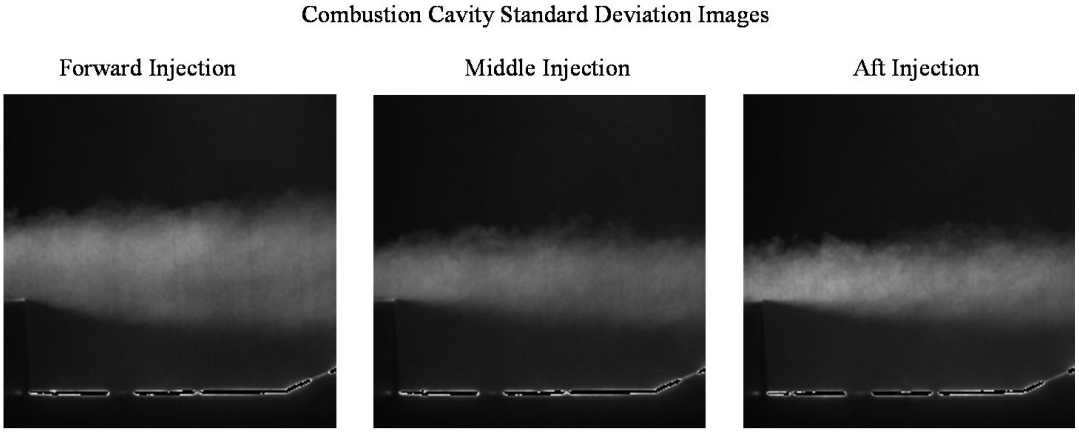

Figure 15. Standard deviation profile images of downstream combustion cavity for each injection location

In the real time analysis of the visual data, both the momentum of the injectant and the flowfield characteristics of the upstream mixing cavity were observed. For upstream wall injection, the transverse momentum of the injectant was the main contributor to injectant escaping into the freestream. However, repeated increases of NO-laden gas entrainment to the freestream were distinguishable and consistent. These volumes of NO-laden gas protruded higher into the freestream and contained higher concentrations of NO. These flow characteristics may have been an indication of a periodic momentum exchange between a trapped vortex and the injectant.

Visual data for the center injection test condition demonstrated the similar periodic shedding of volumes of NO-laden gas. The escape of injectant into the freestream was dominated by the periodic ejection of volumes of injectant. No evidence of the injection momentum leading to escape of the injectant was observed. The shedding of the trapped vortex appeared to be the dominant characteristic of the flowfield.

For injection at the downstream wall, instances of very high NO-PLIF signal are followed by periods of low signal. The shedding and forming of a vortex may have allowed the transverse momentum of the injectant to dominate the flow between cycles dominated by the vortex. As the visual data were non-time correlated, the period of the vortex shedding could not be determined for any test condition.

B. Pressure Analysis

A qualitative analysis of the static pressures measured along the top and bottom walls of the test section were used for estimating pressure losses. The low backpressure condition was once again the area of interest as the static pressure through the test section for the high backpressure setting did not vary with injection pressure. Higher static pressures suggested a stronger shock system which in turn suggested higher total pressure losses.

Static pressures did not vary greatly through the test section based on cavity size, injection location, or injection pressure. The pressures on the bottom wall were nearly identical for each injection pressure. Injection from the floor of the cavity caused a slightly higher static pressure rise, but not enough for exclusion as a solution. The effect of shock reflections from the top wall could be seen downstream of the cavities. Injection pressure did not affect the strength of the first shock. However, the second compression was slightly stronger based on injection pressure, evidenced by a higher static pressure rise. The last static pressure measurement was the same for each injection pressure, leading to the minimum change in pressure loss through the test section based on injection pressure.

The top wall pressures varied slightly due to shocks or expansions impinging at different locations along the wall based on injection pressure. Injection pressure caused a slightly stronger compression from the downstream edge of the upstream cavity. However, the expansion from the leading edge of the combustion cavity is stronger with higher injection pressure. The compression from the ramp of the combustion cavity returns the flow to equal static pressure.

Investigation into the acoustic oscillations created in the upstream mixing cavity showed similar frequencies in both cavities. However, the oscillations were extremely weak and considered irrelevant to the mixing characteristics

of the upstream cavity. The frequencies had amplitudes on the order of 10^{-100} decibels (dB). Fast Fourier Transforms (FFT) displayed many similar amplified frequencies in the spectrums of both the upstream mixing and the downstream combustion cavities. However, the amplitude of these frequencies prevented any one frequency from being considered dominant. All frequency responses were of the same magnitude for each test condition and were too weak to lift any mass through the shear layer into the freestream.

IV. Conclusions

The focus of this mixing study was on the low backpressure or purely supersonic flow condition. Raising the backpressure to create shock-train and supersonic-subsonic mixed flow over in the test section significantly increased the freestream mixing rate of any injection configuration.

The primary and secondary objectives of this research effort were successfully accomplished. Characterizations of the mixing effectiveness of upstream cavities coupled with fuel injection inside the cavity in Mach 2 freestream flow were performed using NO-PLIF as a non-intrusive optical diagnostic technique. Determination of the acoustic characteristics of the upstream and downstream cavities was conducted using high frequency response pressure transducers placed in each cavity. Static pressures were measured throughout the test section for qualitative analysis of the pressure losses of each configuration.

The three mixing cavities each demonstrated the same behaviors inside the test section. Injection at the upstream wall of the cavity created a highly organized and stable plume that diffused the injectant into the freestream. Injection at the center of the cavity demonstrated the strength of the flow inside and over the cavity. Even at the highest injection pressure tested, the injectant did not penetrate into the freestream directly over the injection port. Instead, a layer of injectant spanning the width of the image was observed along with periodic shedding of injectant into the freestream. This band grew into and mixed relatively slowly as the flow moved downstream. Injection at the downstream wall of the cavity was injection pressure dependent. High injection pressures allowed the jet to overcome the trapped vortex flow characteristics and penetrate into the freestream, while some injectant moved upstream in the cavity and forms a band in the shear layer similar to injecting at the center. These two behaviors combine as the flow moves downstream.

The significant concentration and mixing area comparisons demonstrated the relative mixing rate of each injection configuration. Injection at the leading edge of the cavity was observed to have a lower significant concentration area as the flow moved downstream, suggesting greater diffusion of the injectant into the freestream. Injection at this location allowed the injectant to diffuse over a longer distance increasing the effective mixing time with the freestream.

Injection at the center location suggested two possibilities for the behavior of the flow. Injectant may have been suppressed from reaching the freestream, causing less injectant to mix with the flow, or mixing may have taken place inside the cavity with the entrained air and then expelled into the freestream. Most of the injectant from middle injection was located near the test section floor and did not diffuse vertically into the freestream. Injection pressure did not alter this behavior. The flow characteristics in the middle of the cavity were assumed dominant over the injection pressure.

Injection at high enough pressures at the downstream wall of the cavity lead to faster mixing compared to injection at the center of the cavity. The injectant had more transverse momentum compared to injection at the center, allowing the band of injectant to grow faster vertically.

The profile images gave evidence that vortices in the cavity strongly affected the mixing abilities of the flow. Injection at the upstream wall of the cavity took advantage of the natural upward momentum while the vortex dominated the other two injection locations. The ejected vortex did not penetrate into the freestream. Instead, the mass ejected remained near the test section floor and merged with the shear layer.

The qualitative analysis of the static pressure data showed the test configuration did not significantly impact pressure changes. Neither cavity size, nor injection location, nor injection pressure significantly altered the static pressure data to determine a configuration with lower total pressure losses. The high frequency response pressure transducers showed that similar frequency spectra existed in both the upstream and downstream cavities, regardless of cavity dimensions, injection location and injection pressure. However, the amplitude of the frequencies was so low that their effect on mixing was negligible.

Because no great pressure losses could be associated with any one configuration, the injection configuration that best satisfies the needs of the downstream cavity can be chosen. No strong acoustic oscillations were found to be created in the upstream mixing cavity during the experiment and thusly none were carried downstream to the combustion cavity. This eliminates the need to match cavities based on acoustic responses to each other. In this experiment the most effective mixing configuration was the 1.25 in. cavity with injection at the upstream wall.

The results of this investigation showed that the inclusion of an upstream mixing cavity can be used to control the behavior of the injectant interaction with the freestream flow. This may lead to the reduction of injection locations necessary to create efficient combustion in the engine. For instance, the lateral spreading of the injectant from a single injection point on the streamwise centerline of the cavity may be used to mix fuel with the entire span of the combustion chamber. The total pressure losses must be quantified to determine if the inclusion of the cavity provides a benefit or hindrance to the engine.

Acknowledgments

The authors would like to acknowledge the contributions of W. Terry, D. Schommer and H. Meicenheimer for their technical support on this effort. The support of the Air Force Research Laboratory and the Air Force Institute of Technology are also appreciated.

References

[1]McClinton, C.R., Hunt, J.L., Ricketts, R.H., Reukauf, P., Peddie, C.L., "Airbreathing Hypersonic Technology Vision Vehicles and Development Dreams," *9th International Space Planes and Hypersonic Systems and Technologies Conference and 3rd Weakly Ionized Gasses Workshop*, AIAA Paper 99-4978, Norfolk, VA, November 1-5, 1999.

[2]Ben-Yakar, A., and Hanson, R.K., "Cavity Flameholders for Ignition and Flame Stabilization in Scramjets: Review and Experimental Study", AIAA Paper 3122, July, 1998.

[3]Yu. K.H. and Schadow, K.C., "Cavity-Actuated Supersonic Mixing and Combustion Control," *Combustion and Flame*, Vol. 99, pp. 295-301, 1994.

[4]Yu, Ken H., Wilson, Ken J., Schadow, Klaus C., "Effect of Flame-Holding Cavities on Supersonic Combustion Performance", *Journal of Propulsion and Power*, Vol. 17, No. 6, November-December 2001, pp. 1287-1295.

[5]Zhang, X., and Edwards, J.A., "An Investigation of Supersonic Oscillatory Flows Driven by Thick Shear Layers," *Aeronautical Journal*, Vol. 94, No. 919, 1990, pp. 355-364.

[6]Gruber, M.R., Donbar, J.M., Carter, C.D. and Hsu, K-Y., "Mixing and Combustion Studies Using Cavity-Based Flameholders in Supersonic Flow," *Journal of Propulsion and Power*, Vol. 20, No. 5, 2004, pp. 769-778

[7]Gruber, M.R., Baurle, R.A., Mathur, T., and Hsu, K.-Y., "Fundamental Studies of Cavity-Based Flameholder Concepts for Supersonic Combustors," *Journal of Propulsion and Power*, Vol. 17, No. 1, 2001, pp. 146-153.

[8]Zhang, X., and Edwards, J.A., "An Investigation of Supersonic Flow over Two Cavities in Tandem," *AIAA Journal*, Vol. 30, No. 5, 1992, pp. 1182-1190

[9]Gruber, M.R., and Nejad, A.S., "New Supersonic Research Facility," *Journal of Propulsion and Power*, Vol. 11, No. 5, 1995, pp. 1080-1083.

[10]Murugappan, S., Gutmark, E., Carter, C., Donbar, J., Gruber, M., and Hsu, K.-Y., "Control of a Transverse Supersonic Jet Injection into a Supersonic Cross-Stream," *42nd AIAA Aerospace Sciences Meeting and Exhibit*, AIAA Paper 2004-1204, Reno, Nevada, January 5-8, 2004.

[11]Owens, M.G., Mullagiri, S., Segal, C., Ortwerth, P.J., and Mathur, A.B., "Thermal Choking Analyses in a Supersonic Combustor," *Journal of Propulsion and Power*, Vol. 17, No. 3, May-June 2001.

[12]Baurle, R.A., and Eklund, D.R., "Analysis of Dual-Mode Hydrocarbon Scramjet Operation at Mach 4-6.5", *Journal of Propulsion and Power*, Vol. 18, No. 5, September-October 2002.

[13]Mathur, T., and Billig, F., "Supersonic Combustion Experiments with a Cavity-Based Fuel Injector," *Journal of Propulsion and Power*, Vol. 17, No. 6, November-December 2001.

[14]Wood, C.W., Thomas, R.H., and Schetz, J.A., "Effects of Oscillating Shock Impingement on the mixing of a Gaseous Jet in a Mach 3 Air Stream," *26th Joint Propulsion Conference*, AIAA Paper 90-1982, Orlando, Florida, July 16-18, 1990.

[15]Hermanson, J.C., and Winter, M., "Mie Scattering Imaging of a Transverse, Sonic Jet in Supersonic Flow," *AIAA Journal*, Vol.31, No. 1, January 1993, pp. 129-132.

[16]Hill, Philip G., Peterson, Carl R., *Mechanics and Thermodynamics of Propulsion, Second Edition.* Addison-Wesley Publishing Company, New York, 1992, page 21.

[17]Lee, M.P., McMillan, B.K., Palmer, J.L., and Hanson, R.K., "Planar Fluorescence Imaging of a Transverse Jet in a Supersonic Flow," *Journal of Propulsion and Power*, Vol. 8, No. 4, 1992, pp. 729-735.